Defence Science Journal, Vol 46, No 5, November 1996, pp 361-369

Thermal Decomposition Studies of a New, *gem*-Dinitroalkyl Nitramine 1,3,3-Trinitroazetidine (TNAZ)

Richard Behrens, Jr.
Combustion Research Facility, Sandia National Laboratories, Livermore, CA 94551

and

Suryanarayana Bulusu
US Army Armament Research, Development & Engineering Center (ARDEC)
Picatinny Arsenal, NJ 07806-5000

ABSTRACT

The initial results from a study of the thermal decomposition of TNAZ and TNAZ-1-$^{15}NO_2$ using the simultaneous thermogravimetric modulated beam mass spectrometry (STMBMS) technique are presented. The major products formed in the decomposition of TNAZ are NO_2 and NO with slightly lesser amounts of H_2O, HCN, CO/N_2, CO_2/N_2O and 1-nitroso-3,3-dinitroazetidine (NDNAZ). The last mentioned product (NDNAZ) is shown to be an important intermediate in the decomposition of TNAZ and its decomposition has also been examined by synthesizing it independently. Major products formed in this decomposition of NDNAZ are NO with smaller amounts of H_2O, HCN, CO/N_2 and CO_2/N_2O. The temporal behaviours of the ion signals associated with the various thermal decomposition products from TNAZ, TNAZ-1-$^{15}NO_2$ and NDNAZ are also presented. They illustrate the evolution sequence of the various products that are associated with the different reaction pathways that control the decomposition of these materials. In particular, the study of the ^{15}N-labeled sample revealed that NO_2 originates from both the likely sites in the TNAZ molecule and that the cleavage of the nitramine-NO_2 group precedes that of the C-NO_2 cleavage, resulting in similar sequences in the formation of NO and NDNAZ also.

1. INTRODUCTION

TNAZ (1,3,3-trinitroazetidine), (I) is a relatively new energetic material[1] with a strained four membered ring and a *gem*-dinitro group in it. Because of its relatively low m.p. (101 °C) it is melt-castable using steam and is considered to be a useful explosive with valuable applications. Also, TNAZ and mixtures of TNAZ and NDNAZ (1-nitroso-3,3-dinitro-azetidine), (II) are new energetic materials with high energy contents which are considered as possible replacements for HMX and TNT. Understanding the thermal decomposition reactions of these materials is, therefore, important for developing models of their combustion behaviour and their response in abnormal environments. Compared to thermal decomposition studies of the well known cyclic nitramines, RDX and HMX, studies of TNAZ have been new and limited.

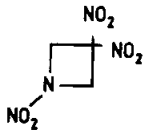

TNAZ (I)

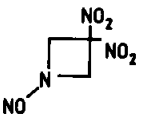

NDNAZ (II)

Received 02 September 1996

Two previous studies of TNAZ have utilized rapid-scan Fourier transform infrared (RSFTIR)[2] technique in the condensed phase and infrared multiphoton dissociation (IRMPD)[3] measurements in the gas phase, to probe the decomposition processes. In the RSFTIR study, based on identification of the lower molecular weight products (i.e., NO_2, *HONO*, *NO*) a mechanism consisting of cleavage of an NO_2 group at either of the *C*-NO_2 or *N*-NO_2 sites, elimination of HNO_2 and a nitro-nitrite rearrangement of the *C*-NO_2 groups was proposed for the decomposition of TNAZ. An uncertainty in this mechanism centers on whether the NO_2 evolves from the nitramine group, the *gem*-dinitro group or both. Another uncertainty was whether the nitro-nitrite rearrangement occurs as postulated, in the condensed phase decomposition.

In the unimolecular decomposition of TNAZ in the molecular beam IRMPD experiments, the results obtained led to the proposal of a mechanism in which the initial step was the loss of NO_2, followed by opening of the ring, subsequent loss of another NO_2 group and then fragmentation of the ring into N_2O_2 and C_3H_4. As in the RSFTIR measurements, there is still an uncertainty as to whether the original NO_2 loss was from the nitramine or *gem*-dinitro group. However, a loss of NO_2 as an initial step in the unimolecular decomposition process is clear from these results.[3]

To develop a reasonable model to characterise the combustion behaviour of TNAZ, it is necessary to characterise the global reaction processes that control its decomposition behaviour. For example, it is not clear whether the first order process as characterised by the results from the IRMPD is also the rate limiting process in a higher pressure environment or whether bimolecular processes should be included to account for other reaction pathways. Furthermore, the appearance of *HONO* in the RSFTIR measurements, suggests that there is another pathway besides the *C*-NO_2 or *N*-NO_2 bond scission. In addition, our previous work on three cyclic nitramines (i.e., RDX[4], HMX[5] and 1,3,5-trinitro-1,3,5-triazacyclo-heptane, TNCHP)[4] suggests that formation of a mono-nitroso analogue of these compounds played an important role in the decomposition. Whether a similar process may be occurring in the decomposition of TNAZ, namely the formation of the nitroso analogue, NDNAZ, is important to determine.

In this paper, we present results of the decomposition of TNAZ and NDNAZ studied by simultaneous thermogravimetry and molecular beam mass spectrometry (STMBMS) measurements that address the issues of the reaction mechanisms raised above, which indeed, may control the decomposition of TNAZ and NDNAZ. We also present the results of the decomposition study of TNAZ-1-$^{15}NO_2$ which shed light on the questions raised. The quantitative gas formation rates of the decomposition products and the associated reaction kinetics are still under investigation.

2. EXPERIMENTAL DETAILS

2.1 Instrument Description

The simultaneous thermogravimetric molecular beam mass spectrometry (STMBMS) apparatus and the basic data analysis procedure have been described previously.[7,8] This apparatus basically consists of a thermobalance, a specially designed alumina reaction cell in which the decomposition is carried out and a quadrupole mass spectrometer with the ionisation source vertically above the reaction cell. In the region between the reaction cell and the ionisation source are located a set of beam defining orifices and a beam-modulating wheel. In the experimental procedure, a small sample (~10 mg) is placed in an alumina reaction cell that is then mounted on a thermocouple probe which is seated on a microbalance. The reaction cell is enclosed in a high vacuum environment (< 10^{-6} torr) and is radiatively heated by a bifilar-wound tungsten wire on an alumina tube. The molecules from the gaseous mixture in the reaction cell exit through a small diameter orifice (2.5 to 970 μ in these experiments, orifice length is 25 μ) in the cap of the reaction cell, traverse two beam-defining orifices before entering the electron-bombardment ioniser of the mass spectrometer where the ions are formed by collisions of 20 eV electrons with the different molecules in the gas flow.

A relatively low electron energy of 20 eV (compared to 70 eV used on normal mass spectrometry measurements) is used to reduce the extent of fragmentation of the higher molecular weight ions and thus, limit their contribution to ion signals measured at lower *m/z* values that are associated with the thermal decomposition products. The background pressures in the vacuum chambers are sufficiently low to eliminate significant scattering between molecules from the reaction cell and background molecules in the vacuum chambers. Different *m/z* value ions are selected with a

quadrupole mass filter and counted with an ion counter. The gas flow is modulated with a chopping wheel and only the modulated ion signal is recorded. This instrument allows the concentration and rate of formation of each gas-phase species in the reaction cell to be measured as a function of time by correlating the ion signals at different *m/z* values measured with the mass spectrometer with the force measured by a microbalance at any instant. The containment time of gas in the reaction cell is a function of the orifice area, the free volume within the reaction cell, and the characteristics of the flow of gas through the orifice. The reaction cell used in the experiments has been described in detail previously[8] and the cap in the reaction cell which showed some leakage of products other than from the orifice, is now sealed effectively using vacuum grease and an O-ring between the taper plug and the gold foil pinhole orifice. The time constant for exhausting gas from the cell is small compared to the duration of the experiments (> 1000 s). Note that the containment time of gas within the reaction cell is short once the gas molecules are in the free volume of the cell, but it may be much longer if the gas is trapped in the condensed phase of the material within the cell. The pressure of the gas products within the reaction cell ranges from less that 1 torr for experiments with the larger diameter orifices (970 μ) to greater than 1000 torr for experiments with the smallest diameter orifices (2.5 μ).

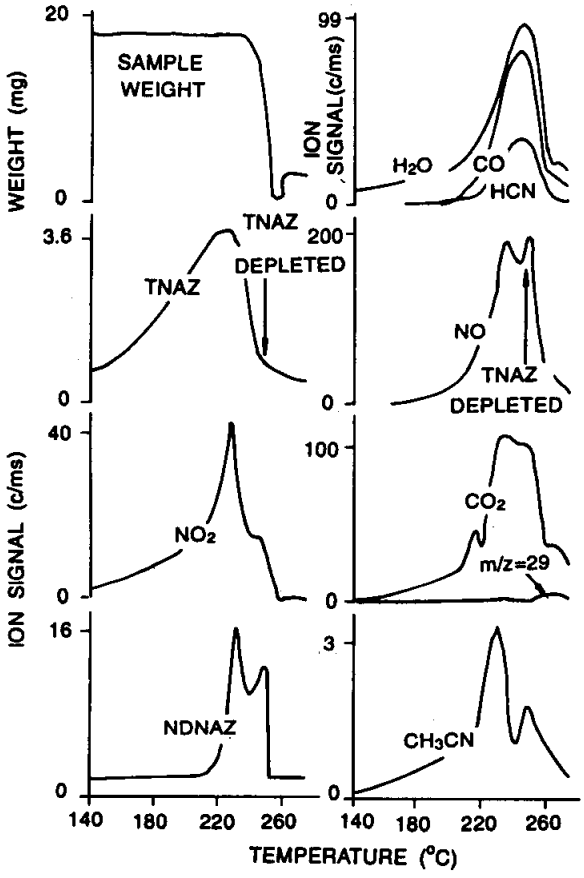

Figure 1. Ion signals representing the major decomposition products from TNAZ. The ion signals have been corrected for the evaporation of TNAZ. The *m/z* values representing each product are: TNAZ (145), NDNAZ (176), NO_2 (46), CO_2/N_2O(44), *NO* (30), CO/N_2 (28), *HCN* (27), CH_3CN (41). Orifice diameter = 2.5 μ, heating rate = 15 °C/min.

2.2 Sample Preparation

The TNAZ was prepared by a previously described method.[1] The $^{15}NO_2$-labeled TNAZ was prepared by treating l-acetyl-3,3-dinitroazetidine with $H^{15}NO_3$. The NDNAZ was obtained from M. Hiskey (Los Alamos National Laboratory). The samples were characterised by NMR and IR measurements. To check whether any impurity evolved from the sample, the sample was evaporated in the STMBMS apparatus prior to conducting the decomposition experiments. The results for TNAZ indicate that it was greater than 99 per cent pure and the results for NDNAZ indicate that there was about 1 per cent TNAZ impurity.

2.3 Data Analysis

The details of the procedure for identifying the pyrolysis products by correlating the temporal behaviour of the various ion signals measured with the mass spectrometer and the analysis of time-of-flight (TOF) velocity spectra have been described previously.[9] The latter technique allows one to determine the neutral precursor of each ion observed in the mass spectrometer and thus discriminate between true thermal decomposition products and electron impact-induced products from evaporating parent compound.

In this paper, we present the qualitative results of the decomposition based on the temporal behaviour of the ion signals measured with the mass spectrometer and associated with the various thermal decomposition products. Because these results are qualitative, strict comparison of the ion signal intensities from one experiment to another can be misleading. However, quantitative results derived from these runs will be presented in a later paper.

3. RESULTS & DISCUSSION

3.1 Identity and Temporal Behaviour of the Decomposition Products from TNAZ

The two major products observed in the decomposition of TNAZ are *NO* (mass spec. ion signal at *m/z*=30) and NO_2 (*m/z*=46). Other major decomposition products observed include: H_2O (*m/z*=18), *HCN* (*m/z*=27), CO/N_2 (*m/z*=28), CH_3CN (*m/z*=41), and NDNAZ (*m/z*=176). Loss of TNAZ itself is monitored by tracking (*m/z*=145) which is an important fragment in the mass spectrum of TNAZ (Table 1). Smaller ion signals are observed at a number of other *m/z* values which will be described in a later publication. The temporal behaviour of both the thermogravimetric analysis (TGA) data and the ion signals representing these major products of TNAZ heated at 15 °C/min in a reaction cell with a 2.5 μ diameter orifice, are shown in Fig. 1. A close examination of the data illustrates the processes that occur during the decomposition of TNAZ. Firstly, TNAZ starts to evolve in significant quantities from the reaction cell at approximately 150 °C as can be seen from the sample weight and the ion signal associated with TNAZ. Even though TNAZ has a relatively high vapour pressure for an energetic material, its rate of evolution from the cell is limited due to the small 2.5 μ orifice diameter used in these experiments. The ion signal associated with TNAZ increases with temperature as its vapour pressure

Table 1. Mass spectra of TNAZ and NDNAZ*

TNAZ		NDNAZ	
Mass	Rel. Intensity (%)	Mass	Rel. Intensity (%)
28	2.1	27	1.5
30	4.2	28	2.9
41	7.0	30	50.2
42	0.6	41	1.4
46	54.5	46	0.7
53	1.0	53	0.6
68	0.7	54	0.8
99	6.5	129	0.6
100	1.4	130	5.5
116	1.1	176	29.3
145	9.9	177	1.5
146	6.8	-	-

* Mass spectra recorded using electron energy of 20 eV.

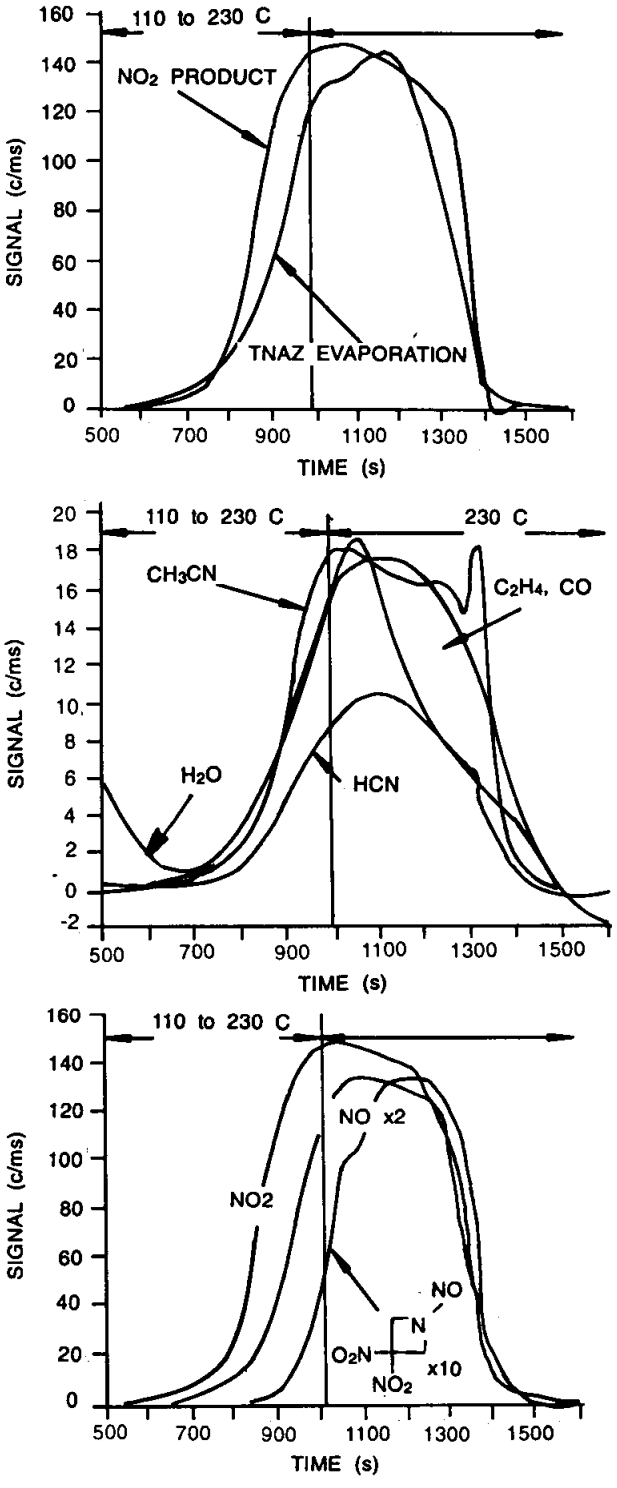

Figure 2. Ion signals representing thermal decomposition products formed from TNAZ heated to 230 °C at 15 °C/min and held there in the reaction cell with 2.5 μ diameter orifice.

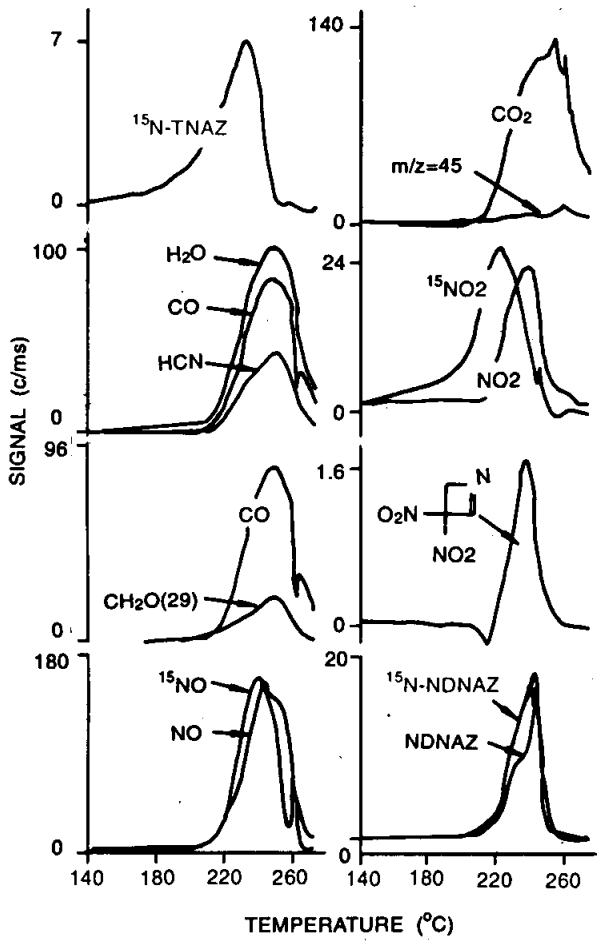

Figure 3. Ion signals representing the thermal decomposition products formed from TNAZ-1-$^{15}NO_2$ heated at 15 °C/min, in a reaction cell with 2.5μ diameter orifice. The products and their *m/z* values are: H_2O(18), HCN(27), CO(28) CH_2O(29), NO(30), ^{15}NO(31), CO_2(44), $^{15}NNO/HCONH_2$(45), NO_2(46), $^{15}NO_2$(47), $C_3H_3N_3O_4$(145), $C_3H_4N_4O_5$ (176) and $C_3H_4{}^{15}N$-N_3O_5(177). The ion signals have been corrected for the contribution of signals from evaporating TNAZ-1-$^{15}NO_2$.

rises until the TNAZ in the reaction cell is depleted as shown in Fig. 1. Secondly, examination of the ion signal representing NO_2 shows that its evolution commences at approximately 140 °C, reaches a peak at 230 °C and then decreases. This behaviour is consistent with a reaction that is first order in TNAZ because the rate of decomposition of TNAZ to NO_2 increases with temperature and then decreases as the amount of TNAZ in the reaction cell decreases. This behaviour also indicates that TNAZ is decomposing in both the liquid

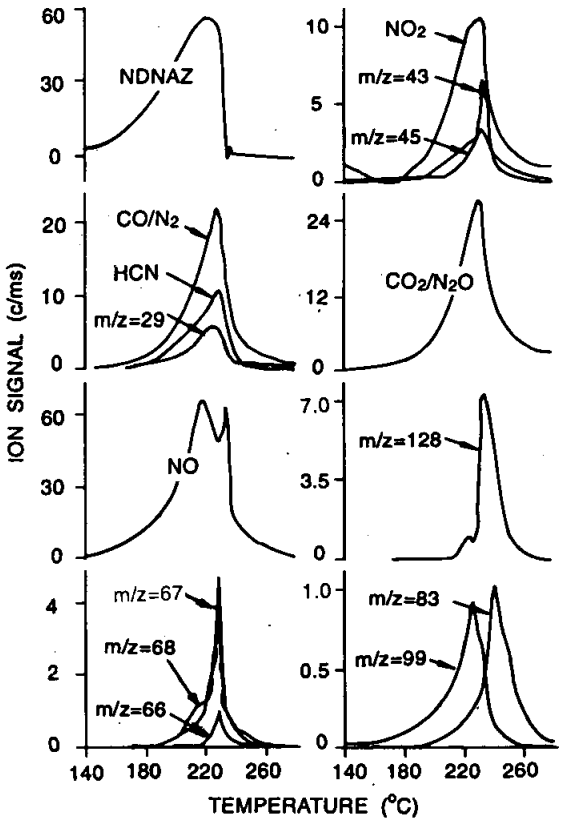

Figure 4. Ion signals representing the major decomposition products from NDNAZ. The ion signals have been corrected for the evaporation of NDNAZ. The *m/z* values representing each product are: NDNAZ(176), HCN(27), CO/N_2(28), NO(30), NO_2(46), and CO_2/N_2O (44). Reaction cell orifice diameter, 2.5μ ; heating rate, 15 °C/min.

and gas phases since the rate of NO_2 formation is proportional to the total amount of TNAZ in the cell and not just the amount of TNAZ in the gas phase (which continues to increase until it nears depletion). Thirdly, the evolution of the signals at *m/z* values 44 (CO_2), 176 (NDNAZ), 30 (NO), 28 (CO or N_2), 27 (HCN) and 41 (CH_3CN) continues beyond the temperatures (and times) corresponding to the evolution of NO_2 and also TNAZ itself. This indicates that another reaction pathway competes with the direct decomposition of TNAZ to NO_2 and other low molecular weight gas phase products, as observed in the RSFTIR and IRMPD experiments.

The formation of the mononitroso analogue of TNAZ, namely NDNAZ, in the decomposition of TNAZ appears to be the other major reaction pathway as will be shown in the following discussions. Formation of the nitrosamine (N-NO) from the nitramine (N-NO_2) group

is shown to play an important role in controlling the decomposition pathway similar to the other cyclic nitramines (i.e., RDX, HMX and TNCHP). Decomposition through the mononitroso intermediate is consistent with several of the features of the data shown in Fig. 1. For example, NDNAZ first appears at about 200 °C and increases as the amount of *NO* increases, suggesting that *NO* reacts with TNAZ to form NDNAZ. The fact that the NDNAZ signal decreases as the amount of TNAZ decreases is also consistent with a direct reaction with *NO*. The increase in the NDNAZ signal as the TNAZ in the cell nears depletion is consistent with an increasing mole fraction of NDNAZ in the liquid phase and the resulting increase in its partial pressure in the reaction cell. Finally, evolution of CO_2/N_2O, *NO*, *HCN* and CO/N_2 after the depletion of TNAZ suggests that they are the thermal decomposition products from NDNAZ.

The results from an isothermal decomposition experiment with TNAZ also support a reaction mechanism consisting of parallel reaction pathways. These results at 230 °C are shown in Fig. 2. The m/z values representing each decomposition product are: TNAZ (145), NDNAZ (176), NO_2 (46), *NO* (30), $CO/N_2/C_2H_4$ (28), *HCN* (27), CH_3CN (41). The ion signals have been corrected for the contribution of signal from evaporating TNAZ. NO_2 is an abundant decomposition product and its rate of formation falls as the amount of TNAZ falls. However, the ion signal associated with NO_2 (m/z=46) does not fall as rapidly as the ion signals associated with H_2O and *HCN*. This suggests that H_2O and *HCN* originate from reactions associated with a decomposition reaction that is first order in the total TNAZ in the reaction cell (both phases), whereas, NO_2 may originate from more than one source. The formation of NDNAZ from TNAZ is also clearly illustrated in Fig. 2. First an increase in the rate of formation of NO_2 is observed, followed by a rise in the rate of formation of *NO* and finally a rise in the rate of formation of NDNAZ. This is reminiscent of the RDX decomposition[3] in which NO_2 is replaced by *NO* to form the nitrosamine, ONDNTA. The behaviour of NO_2, *NO* and NDNAZ from TNAZ is, therefore, consistent with a mechanism analogous to the one that gives ONDNTA from RDX. This suggests that the nitramine NO_2 group is replaced by *NO* in TNAZ also to form the nitrosamine analogue, as in the case of RDX.

3.2 Thermal Decomposition of TNAZ-1-$^{15}NO_2$

Figure 3 presents the ion signals obtained from the decomposition of TNAZ-1-$^{15}NO_2$ heated at 15 °C/min. The most interesting differences between these signals and those obtained from unlabelled TNAZ (Fig. 1) are first, the appearance of both $^{15}NO_2$ and NO_2 signals which are of nearly equal intensity and uncorrelated. Likewise, there are separate signals each for $^{15}NO/NO$ and ^{15}N-NDNAZ/NDNAZ, also uncorrelated and of equal intensity. This clearly suggests that NO_2 is formed from both the possible sites in the TNAZ molecule, namely, the nitramine group and the *gem*-dinitro group, but the former precedes the other significantly earlier. However, the time lags between the ^{15}N-labelled and unlabelled species of *NO* and NDNAZ are much smaller than for NO_2. The thermal decomposition product, m/z = 145 (193- 48) presumably derives from elimination of $H^{15}NO_2$ exclusively from the nitramine function and an adjacent *H* but not from the C-NO_2 function analogous to the previous nitramines studied. The earlier conclusion that the nitroso-DNAZ is derived by a reattachment of ^{15}NO or *NO* to the initial radical produced by the loss of nitramine-NO_2 is borne out by the correlations of $^{15}NO/NO$ and ^{15}N-NDNAZ / NDNAZ.

It is apparent from an examination of the ^{15}N and unlabelled species shown in the plots of Fig. 3 that NO_2 originates from both the possible sites in the TNAZ molecule and that the cleavage of the nitramine-NO_2 precedes that of the C-NO_2 cleavage. This also results in similar sequences of $^{15}NO/NO$ and ^{15}N-NDNAZ/NDNAZ. This observation is consistent with the fact that N-NO_2 bond is weaker than C-NO_2 bond. Once an N-NO_2 bond cleaves, other C-NO_2 bonds can cleave more readily as predicted by the calculations of Melius[10]. It is also worth mentioning that the lack of ^{15}N-isotopic shifts show that m/z = 44 and m/z = 28 are predominantly CO_2 and *CO*, respectively and not N_2O and N_2.

3.3 Thermal Decomposition of Independently Synthesized NDNAZ

The thermal decomposition of NDNAZ is controlled by a complex process that forms both gas-phase and liquid-phase products. Ion signals associated with thermal decomposition products formed from NDNAZ are shown in Fig. 4 for a 12 mg sample of NDNAZ heated at 15 °C/min in a reaction cell with a 2.5 μ diameter orifice. The vapour pressure of NDNAZ is relatively high as can be seen from the large ion signal

associated with the evaporation of NDNAZ in Fig. 4. The NDNAZ in this experiment is depleted when the sample reaches a temperature of ~ 235 °C. Examination of the ion signals associated with the thermal decomposition products show continued evolution from the reaction cell after the NDNAZ is depleted. This suggests that products with low volatility are formed in liquid-phase during the decomposition and their evolution and decomposition continues as the sample is heated further

Table 2. Probable composition of the unidentified m/z species in Fig. 4

m/z	$C_3H_4N_4O_5$(NDNAZ)	Composition
66	176 - 110 ($2HNO_2 + O$)	$C_3H_2N_2$
67	176 - 109 ($HNO_2 + NO_2 + O$)	$C_3H_3N_2$
68	176 - 108 ($2NO_2 + O$)	$C_3H_4N_2$
83	176 - 93 ($HNO_2 + NO_2$)	$C_3H_3N_2O$
99	176 - 77 ($HNO_2 + NO$)	$C_3H_3N_2O_2$
128	176 - 48 ($NO + H_2O$)	$C_3H_2N_3O_3$

NDNAZ decomposes at significant rates in these experiments starting at approximately 160 °C as indicated by the first appearance of the ion signals associated with the thermal decomposition products. The rates of formation of several of the lower molecular weight gaseous products, such as CO/N_2 and HCN, fall to zero as the NDNAZ sample is depleted indicating that they are formed directly from the decomposition of NDNAZ. In contrast, some products start evolving at a higher temperature and also fall-off as the NDNAZ is depleted. For example, a product associated with ion signals at m/z values of 66, 67 and 68 starts appearing at approximately 180 °C and its rate of formation increases rapidly at ~ 210 °C. Further, other products start evolving at a higher temperature and continue to evolve after the NDNAZ is depleted. Examples of this behaviour are seen with the CO_2/N_2O signal and ion signals representing a number of different products at m/z values of 43, 83, 99 and 128. In the case of the product represented by the m/z = 128 signal, the rate increases significantly after the NDNAZ is gone.

The identities of the thermal decomposition products from NDNAZ are similar to those formed in the decomposition of TNAZ. However, the relative amounts of the major products differ significantly. The other most abundant thermal decomposition products from NDNAZ are H_2O, HCN, CO/N_2, CO_2, NO_2 and some of the less volatile products that remain in the liquid phase, parallel to the behaviour of TNAZ. The identities of the thermal decomposition products associated with the ion signals of various m/z values shown in Fig. 4 require conducting TOF velocity spectra measurements which will be carried out in the future.

3.4 Basic Reaction Pathways for TNAZ

From the STMBMS measurements on TNAZ we have observed that the products are consistent with the direct decomposition mechanisms proposed based on previous RSFTIR measurements[2] and unimolecular IRMPD measurements[3]. In addition, we observed the new reaction product, NDNAZ, which shows that the reaction pathways other than the unimolecular decomposition alone must be considered in developing a mechanism for the thermal decomposition of TNAZ. The first step in the decomposition of TNAZ appears to be N-NO_2 and C-NO_2 bond homolysis, replacement of the nitramine NO_2 group with an NO group and the possible nitro- nitrite rearrangement of NO_2 at the *gem*-dinitro group. These steps are summarized as follows:

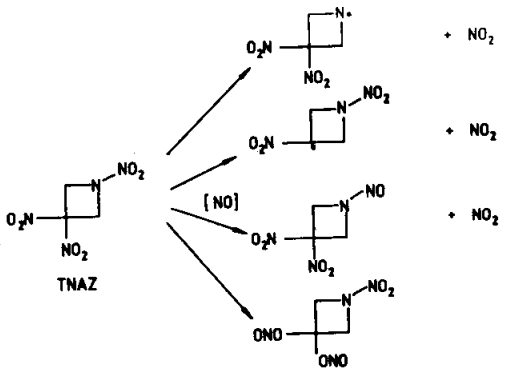

The NO required for the conversion of TNAZ to NDNAZ may form through either the nitro-nitrite rearrangement reaction, and the reaction of NO with CH_2O or via the loss of N_2O_2 after the NO_2 loss and the ring opening steps in the IRMPD mechanism. Once the nitroso analogue of TNAZ is formed, it alters the subsequent decomposition pathway by significantly reducing the direct decomposition to NO_2 and enhancing

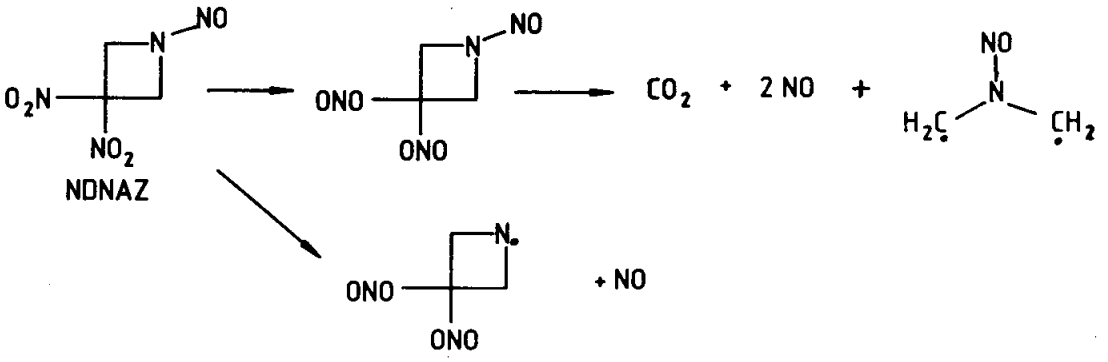

the rate of formation of *NO*. Two possible pathways for producing *NO* from NDNAZ are as follows:

The fact that the rate of formation of *NO* compared to NO_2 is significantly higher in the thermal decomposition of NDNAZ indicates that a nitro-nitrite rearrangement reaction is more likely for the nitrosamine than the nitramine. The formation of *NO* by scission of *N-NO* bond probably occurs but it cannot account for the significant increase of *NO* formed in the decomposition.

The ion signals observed in the decomposition of NDNAZ (Fig. 4) also include several unassigned mass species in the *m/z* range 66-128. Given the fact that there are only four possible atomic species (*C, H, N,* and *O*), one can speculate on the possible atomic compositions of these species as summarised in Table 2. The identities of the species in the last column will be established with the help of isotopic shifts using ^{15}N-labelled material and time of flight velocity data both of which are currently being obtained.

The mass spectrometry data on the thermal decomposition of TNAZ and NDNAZ clearly show many ion signals at different *m/z* values associated with products of secondary reactions. Several of the products come directly from the ring *HCN* (*m/z* = 27) and CH_3CN (*m/z* = 41). Others such as H_2O and CO/N_2 come from secondary reactions of thermal decomposition products, while many other ion signals have not yet been associated with specific thermal decomposition products since further information is required to make these assignments.

It is clear from the STMBMS results that the construction of a realistic mechanism to characterise the thermal decomposition process of TNAZ requires the use of several parallel reaction pathways. Construction of a useful model of the decomposition process requires measuring the temperature-dependent rate constants for each of these pathways.

3.5 Further Work

The work on the thermal decomposition of TNAZ and NDNAZ presented in this paper is the first step of examining the decomposition of these materials with the STMBMS technique. Further work on TNAZ will include making TOF velocity spectra measurements of the various ion signals to determine the identities of the secondary products. Quantitative analysis of the data will be made to determine the gas formation rates of the different products as a function of time. Finally, the time and temperature dependence of the gas formation rates of the different products will be analysed to determine the temperature dependence of the rate constants for the different reaction pathways.

4. SUMMARY

The results presented in this paper on the decomposition of TNAZ show that its thermal decomposition is controlled by a number of different competitive and coupled reactions. The formation of NO_2 is consistent with either $C\text{-}NO_2$ and/or $N\text{-}NO_2$ bond homolysis and is in agreement with the pathways determined in the IRMPD experiments. This study shows that in the presence of decomposition products TNAZ reacts with *NO* to form the nitroso analogue of TNAZ, NDNAZ. The temporal behaviours of the decomposition products show that as the amount of NDNAZ increases in the TNAZ sample, new products associated with the decomposition of NDNAZ appear and contribute to an increase in the overall decomposition of TNAZ. Thus, to adequately characterise even the first step of the decomposition process, bimolecular reactions must be

included. The first decomposition products from TNAZ were observed at ~ 160 °C in the STMBMS experiments and the formation of NDNAZ was first observed starting at ~ 200 °C. Decomposition products associated with NDNAZ were observed after all of the TNAZ was thereby consumed suggesting that NDNAZ is thermally more stable than TNAZ.

The decomposition of NDNAZ shows that changing the *N-NO2* group to *N-NO* group alters the decomposition process. For NDNAZ a much larger proportion of *NO* as compared to NO_2 is formed in the decomposition process. This may be due to an enhanced propensity to undergo nitro-nitrite rearrangement that leads to the formation of *NO* and the elimination of CO_2 from the azetidine ring. This is consistent with the results. The decomposition of NDNAZ produces both volatile gaseous products and some products that remain in the liquid phase.

The temporal behaviour of the product species from the thermal decomposition of both TNAZ and NDNAZ indicates that the reactions occur in both the gas and liquid phases.

Further STMBMS experiments and analyses will be conducted to identify other reaction products, obtain more details on the reaction pathways and determine the temperature-dependent rate constants for the different pathways. These experiments are also expected to shed light on the effect of the *gem*-dinitro group on the thermal stability of TNAZ relative to other cyclic nitramines.

ACKNOWLEDGEMENT

We would like to acknowledge the help of David Puckett for collecting the experimental data and to Dr. Michael Hiskey for providing the NDNAZ.

REFERENCES

1. Archibald, T. G.; Gilardi, R.; Baum, K. & Cohen, M. C. *J. Org. Chem.*, 1990, **55**, 2920.

2(a). Oyumi, Y. & Brill, T. B. *Combust. Flame*, 1985, **62**, 225.

2(b). Oyumi, Y. & Brill, T.B. *Combust. Flame*, 1987, **68**, 209.

3. Anex, D. S.; Allman, J.C. and Lee, Y.T., In Chemistry of energetic materials, edited by G.Olah. Academic Press, New York, 1991. p. 27.

4. Behrens, Jr. R. & Bulusu, S. J. *Phys. Chem.*, 1992, 96, 8877 & 8891.

5(a). Behrens, Jr. R. *J. Phys. Chem.*, 1990, **94**, 6706.

5(b). Behrens, Jr. R. & Bulusu, S. *J.Phys. Chem.*, 1991, **95**, 5838.

6 Behrens, Jr. R. & Bulusu, S. *Mater. Res. Soc. Symp. Proc.*, 1993, **296**, 13.

7(a). Behrens, Jr. R. *Rev. Sci. Instrum.*, 1986, **58**, 451.

7(b). Behrens, Jr. R. The application of simultaneous thermogravimetric modulated beam mass spectrometry and time-of-flight velocity spectra measurements to the study of the pyrolysis of energetic materials. *In* Chemistry and physics of energetic materials, edited by S.N.Bulusu, Proceedings of the NATO Advanced Study Institute, Kluwer Academic Publishers, Netherlands, 1990, 309, p. 327.

8. Behrens, Jr. R. *Int. J. Chem. Kinetics*, 1990, **22**, 135.

9. Behrens, Jr. R., Int. J. Chem. Kinetics, 1990, **22**, 159.

10. Melius, C. F. and Binkley, J. S. *In* Proceedings of the 21st Symposium (International) on Combustion, 1987, The Combustion Institute, Pittsburgh, PA, 1988.